Arabian Journal for Science and Engineering (2019) 44:949–957
https://doi.org/10.1007/s13369-018-3312-1

RESEARCH ARTICLE - MECHANICAL ENGINEERING

Effect of First and Second Passes on Microstructure and Wear Properties of Titanium Dioxide-Reinforced Aluminum Surface Composite via Friction Stir Processing

Vikram Kumar S. Jain[1] · James Varghese[1] · S. Muthukumaran[1]

Received: 16 November 2017 / Accepted: 17 May 2018 / Published online: 6 June 2018

Abstract
The dispersion of particles in polymer, ceramic and metal matrix composites via conventional routes was very difficult, due to agglomeration/clustering of particles, poor compatibility of properties of particle and matrix. So, an attempt has been made to uniformly disperse the titanium dioxide particles on the surface of aluminum matrix via two-pass friction stir processing. The effect of passes on particle distribution, microstructure, microhardness and wear properties was systematically investigated. Microstructural studies revealed a fine equiaxed grain structure in the stir zone due to the dynamic recrystallization. The first-pass surface composite sample results in agglomeration of particles toward the advancing side due to insufficient materials flow and strain. The second pass was carried out by changing advancing and retreating side of composite plate processed by the first pass. The results showed that marginal change in grain size was observed with homogeneous microstructure when compared to first-pass surface composite. Microhardness was carried out across the cross sections of the surface composites to obtain hardness profile. The tribological performance was assessed using a pin-on-disk tribometer. The result reveals that surface composites processed by the second pass show better hardness and wear resistance when compared to as-received aluminum. The wear mechanism shows a transition from adhesive wear in surface composites to the combination of abrasive and delamination wear in as-received aluminum.

Keywords Friction stir processing · Aluminum · Titanium dioxide · Microhardness · Wear rate · Surface composite

1 Introduction

The Welding Institute (TWI), UK, invented friction stir welding (FSW) process in 1991, initially for joining of aluminum and its alloys [1]. Aluminum and its alloys are commonly used in various engineering applications such as aircraft, automobiles, transportation and marine hulls, because of its excellent properties such as high strength to weight ratio, stiffness, wear and corrosion resistance. The non-weldable aluminum alloys such as 2000 and 7000 series can easily be welded using FSW process in comparison with conventional fusion welding processes. FSW process is a viable method of joining of materials and is eco-friendly, energy and cost efficient [2]. Soon after the invention of FSW process, the scientific community across the world applied this process for joining of similar and dissimilar materials [3–8]. Friction stir processing (FSP) method is based on the principle of FSW, and FSP was applied to modify the microstructure of materials. FSP is a newly evolved severe plastic deformation process (SPD) where plastic deformation occurs by forcibly plunging a revolving non-consumable tool into the workpiece and transverse toward the particular direction [9]. Researchers and scientists widely used FSP process for the fabrication of surface composites which exhibits excellent mechanical and tribological properties with respect to monolithic materials. Ranjit et al. [10] applied multiple FSP passes on as-cast Al–TiC composite to eliminate the casting defects and improve the particles distribution. Shahi et al. [11] fabricated the surface composites by the addition of nickel powder particles into the commercially pure aluminum. As the number of FSP passes increases from 2 to 6 with different rotational speed and traverse speed, there is a formation of intermetallic compounds (Al_3Ni). Choi

✉ S. Muthukumaran
smuthu@nitt.edu

[1] Department of Metallurgical and Materials Engineering, National Institute of Technology, Tiruchirappalli, Tamil Nadu 620 015, India

et al. [12] reported that SiC particles were uniformly distributed in the Al6061-T4 matrix via FSP. The addition of SiC particles in Al6061-T4 matrix attributes to grain refinement when compared to FSPed Al6061-T4 alloy. Adel et al. [13] developed Al/$Al_2O_3-Al_3Ni$ hybrid nanocomposites by reinforcing NiO particles (less than 1 μm) with aluminum matrix via friction stir processing. Alidokht et al. [14] fabricated A356 hybrid surface composite layer by reinforcing SiC and MoS_2 particles via FSP. The addition of SiC particles in the matrix improves hardness and wear resistance, whereas MoS_2 particles in matrix act as a solid lubricant and prevent metal to metal contact. Yuvaraj et al. [15] studied wear behavior of mono- and hybrid nanocomposite by FSP. For better dispersion of particulates in Al matrix alloy, three FSP passes were carried out at a rotational speed of 1000 rpm and transverse speed of 40 mm/min. Sakari et al. [16] investigated the influence of multiple FSP passes on the distribution of the nano-SiC particles with the simple cylindrical probe and threaded cylindrical probe. The results showed that simple cylindrical probe exhibits appropriate distribution of particles which required at least three FSP passes to be carried out without changing the same rotational direction. The threaded cylindrical probe with changing of rotation direction between the passes exhibits an acceptable distribution of particles. Zihao et al. [17] reported a surface modification of Ti–6Al–4V alloy was carried out via FSP by introducing TiO_2 particles to strengthen the material as well as for biomedical application.

Although, some literature was available with respect to the dispersion of the particles via multiple passes. During the multiple passes, more heat will be generated which may induce intermetallics phases, and coarsening of grain takes place which affects mechanical and tribological properties. However, as far as the authors' knowledge is concerned, there is no work carried out on titanium dioxide-reinforced aluminum surface composite by two-pass FSP. The effect of passes on particle distribution, microstructure, microhardness and wear properties was systematically studied. The tool geometry was self-optimized and played an important role in particle distribution and material flow. The first pass was carried over the empty pass, which was used to enclose the holes on the surface of the aluminum plate. The second pass was carried over the first pass by changing advancing and retreating side of the parent metal. The microstructure of composite layers was examined through an optical microscope, scanning electron microscope. Microhardness testing was conducted across cross sections of the surface composite, and sliding wear test was carried out on pin-on-disk tribometer as per ASTM standards G-99-05.

2 Experimental Procedure

Commercially pure aluminum (AA1050 grade with 99.5% purity) plate of 6 mm thickness was chosen as starting material was purchased from PMC Corporation, India. The holes

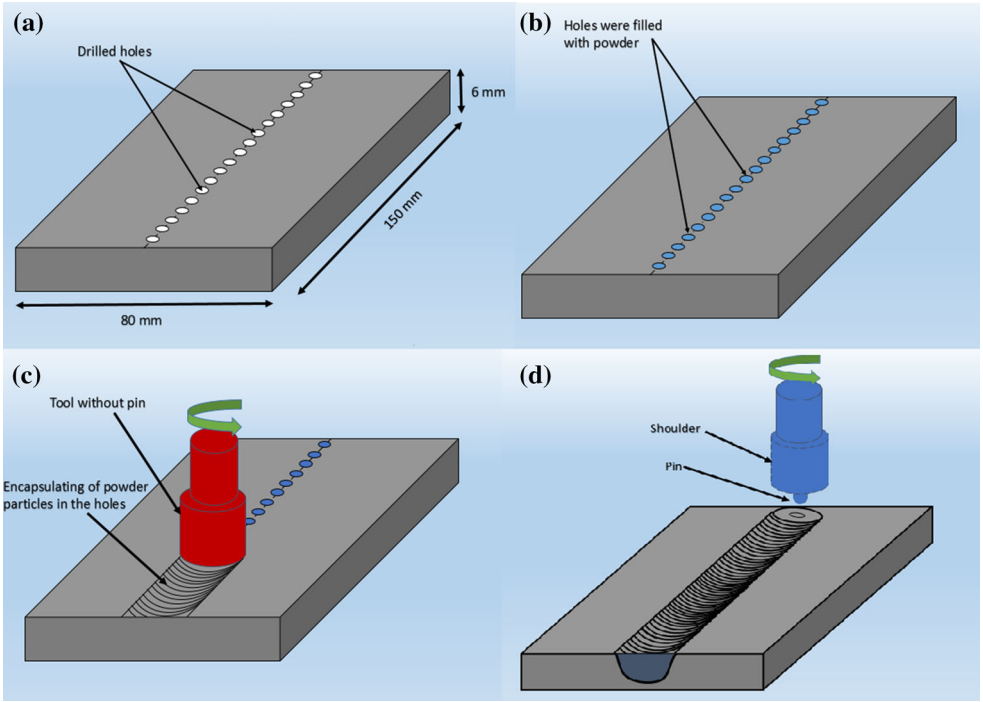

Fig. 1 Schematic of fabrication of surface composite **a** drilled holes, **b** holes filled with TiO_2 particles, **c** encapsulating of particles into holes with pin-less tool, **d** first FSP pass with pin-tool

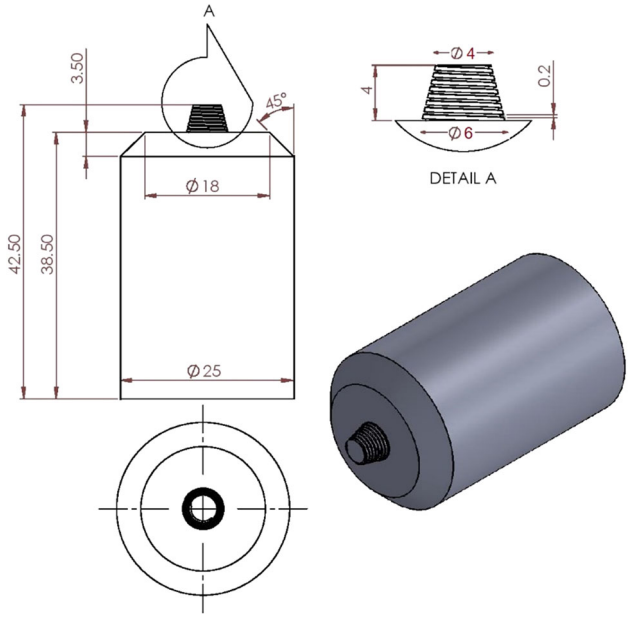

Fig. 2 Schematic illustration of FSP tool (dimensions in mm)

were machined on an aluminum plate with a diameter of 2.5 mm to a depth of 3 mm for every 3 mm interval as shown in Fig. 1a. The TiO_2 particles (procured from Merck India, Anatase phase with $\geq$ 99.95% purity) were incorporated into the holes as shown in Fig. 1b. The holes filled with particle were enclosed by empty pass to inhibit the escape of particles as shown in Fig. 1c. Then, a specially designed tool with a pin and shoulder was used to carry out FSP as shown in Fig. 1d. TiO_2 particles have higher hardness, low coefficient of thermal expansion, higher wear resistance and good wettability [18]. The schematic representation of FSP tool is shown in Fig. 2.

The FSP was performed on a 4-axis numerically controlled FSW machine (BISS, India) with process parameters such as rotational speed of 1600 rpm, traverse speed of 20 mm/min and tool tilt angle of 3° degrees. The parameter was selected based on the experimental trails to obtain defect-free stir zone [19]. The tool with shoulder diameter of 18 mm, pin length of 4 mm and taper threaded pin profile was selected for the present study based on self-optimized tool geometry recommended by Prado and Murr [20]. The first pass was carried over the empty pass as shown in Fig. 3.

The second pass was carried over the first pass by changing advancing and retreating side of the friction stir-processed (FSPed) plate. The microstructural investigation was carried out using an optical microscope and scanning electron microscope. The base metal and FSPed samples were polished with different grades of emery sheets, and mirror-like finish was obtained by using diamond paste (0.5 μm) on the disk polishing machine as per standard metallographic techniques. The etchant used for samples was modified Poulton's reagent. The grain size was calculated using a linear intercept method as per the ASTM standards 112-96. Microhardness test was performed on cross-sectioned samples perpendicular to the processed region using Vickers microhardness tester (Wolpert Wilson) with a load of 0.1 kgf and dwell time of 15 s. The dry sliding wear test was performed on pin-on-disk tribometer (DUCOM TR20-LE, Bengaluru, India) as per ASTM G99-05. The samples of 4 mm*4 mm*20 mm were prepared from the base metal and FSPed region by using wire EDM. The counter disk was made of EN31 steel material which has a hardness of 63 HRC. The dry sliding wear test was carried out at a load of 20 N, sliding speed of 1 m/s and sliding distance of 1000 m. The volumetric loss was calculated by multiplying the cross section of the pin sample with its loss of height. The wear rate was assessed by volumetric loss of samples to sliding distance.

3 Results and Discussion

3.1 Microstructural Characterization

The micrographs of first-pass aluminum without reinforcement are shown in Fig. 4, in which different zones were observed. This zone includes friction stir zone (FSZ), thermo-mechanically affected zone (TMAZ) and heat-affected zone

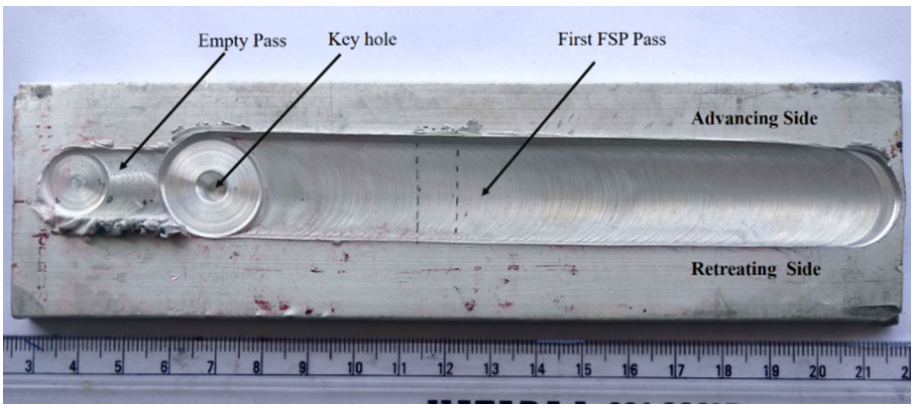

Fig. 3 Top view of FSPed aluminum-reinforced TiO_2 plate (first pass)

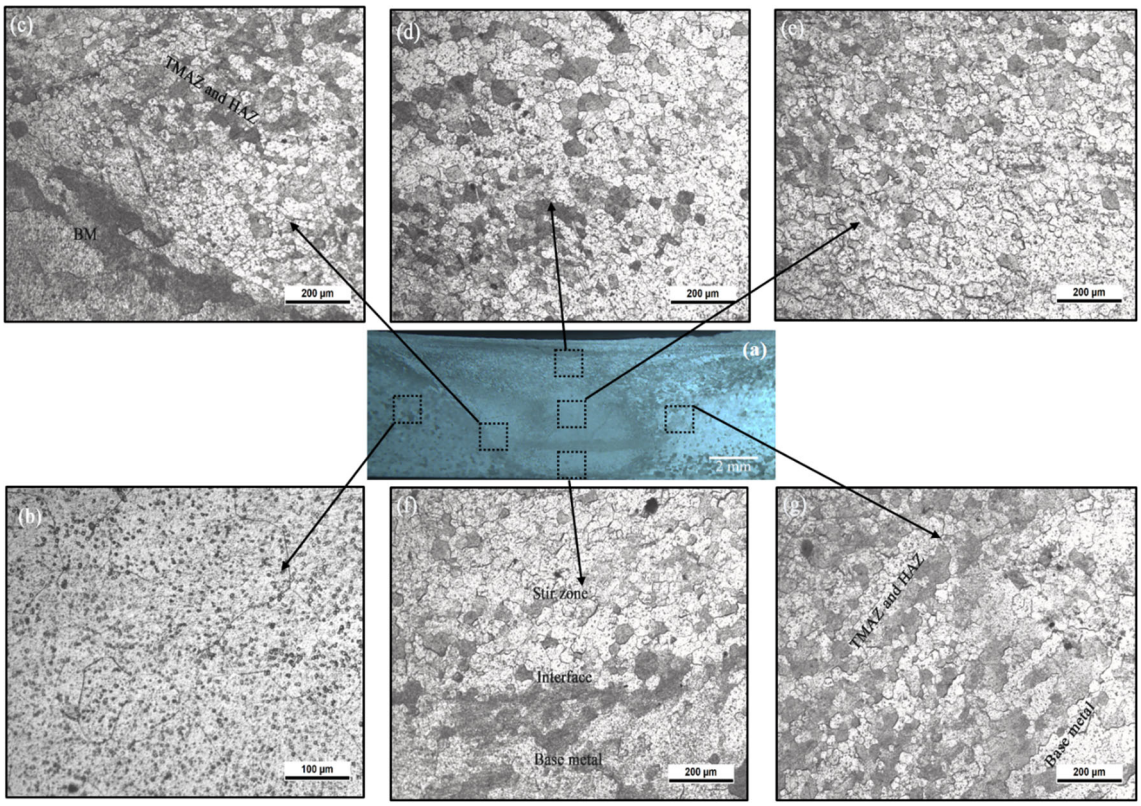

Fig. 4 Optical micrographs of FSPed aluminum without TiO_2 particles **a** macrograph, **b** BM, **c** TMAZ on retreating side, **d** upper region of the FSZ, **e** middle region of the FSZ, **f** bottom region of FSZ, **g** TMAZ on advancing side

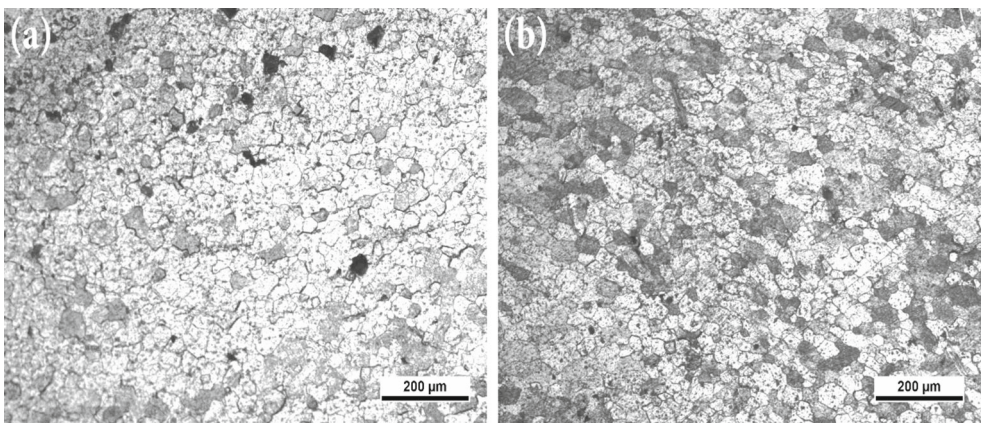

Fig. 5 FSPed aluminum-reinforced TiO_2 particles **a** first pass, **b** second pass

(HAZ). The FSZ exhibits finer equiaxed grains than that of the parent metal. The grain refinement was significantly stimulated by dynamic recrystallization (DRX) through severe plastic deformation. It occurs because the effect of revolving tool shoulder touches the substrate, in turn, producing frictional heat which plasticizes the material and action of the tool pin promote stirring of the parent metal. The dynamic recrystallization of aluminum and its alloy involves a continuous dynamic recrystallization process (CDRX). The TMAZ undergoes deformation, but temperature required for recrystallization is insufficient. The materials flow causes grains to elongate around the revolving pin. The HAZ experiences the thermal cycle and does not deform. Hence, grain coarsening takes place. The grain size analyses were carried out on parent metal and FSPed samples using image analysis software as per ASTM standards 112-96. The grain size of parent metal was measured and found to be 42.85 µm. After the first pass without reinforcement, the grain size was reduced

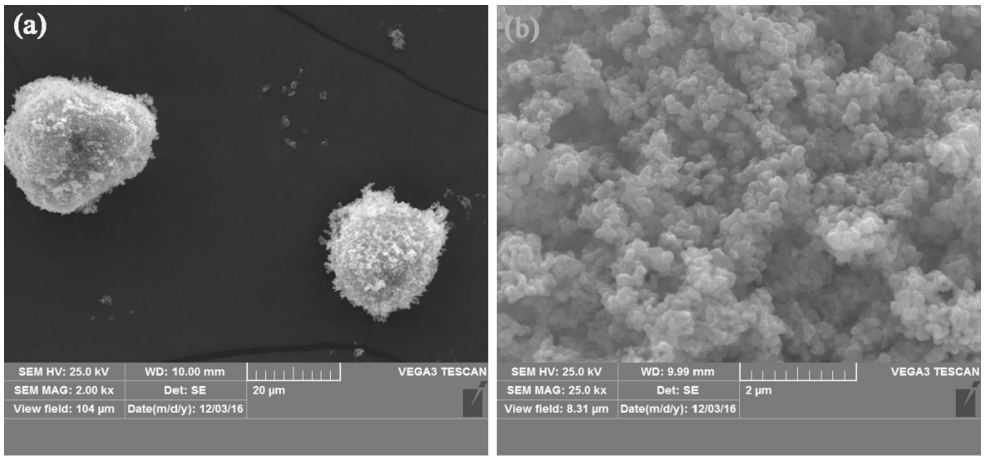

Fig. 6 SEM micrograph of TiO_2 particles at **a** lower, **b** higher magnification

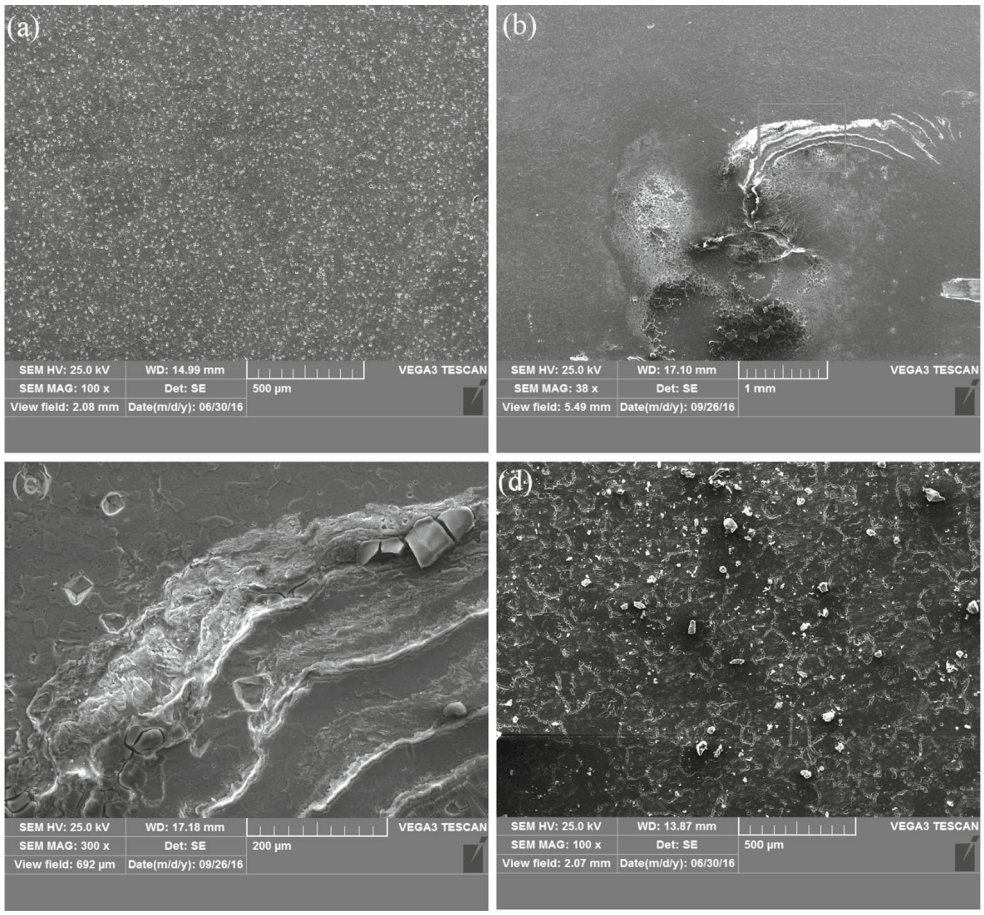

Fig. 7 SEM micrograph of FSPed **a** aluminum without TiO_2 particles, **b** aluminum with TiO_2 particles, **c** enlarged view of agglomerated particles in the stir zone (**b**), and **d** second pass (aluminum with TiO_2 particles)

to 10.58 µm. The grain size of the first pass and second pass with reinforcement was found to be 5.0 and 4.5 µm. Figure 5 depicts the stir zone of first- and second-pass surface composites. Figure 6a, b shows the SEM micrograph of TiO_2 particles at lower and higher magnification. The average particle size was found to be 20–30 µm.

Figure 7a shows the first pass without reinforcement. Figure 7b, c shows the first pass with reinforcement. Most of the TiO_2 particles are agglomerated within the stir zone (SZ)

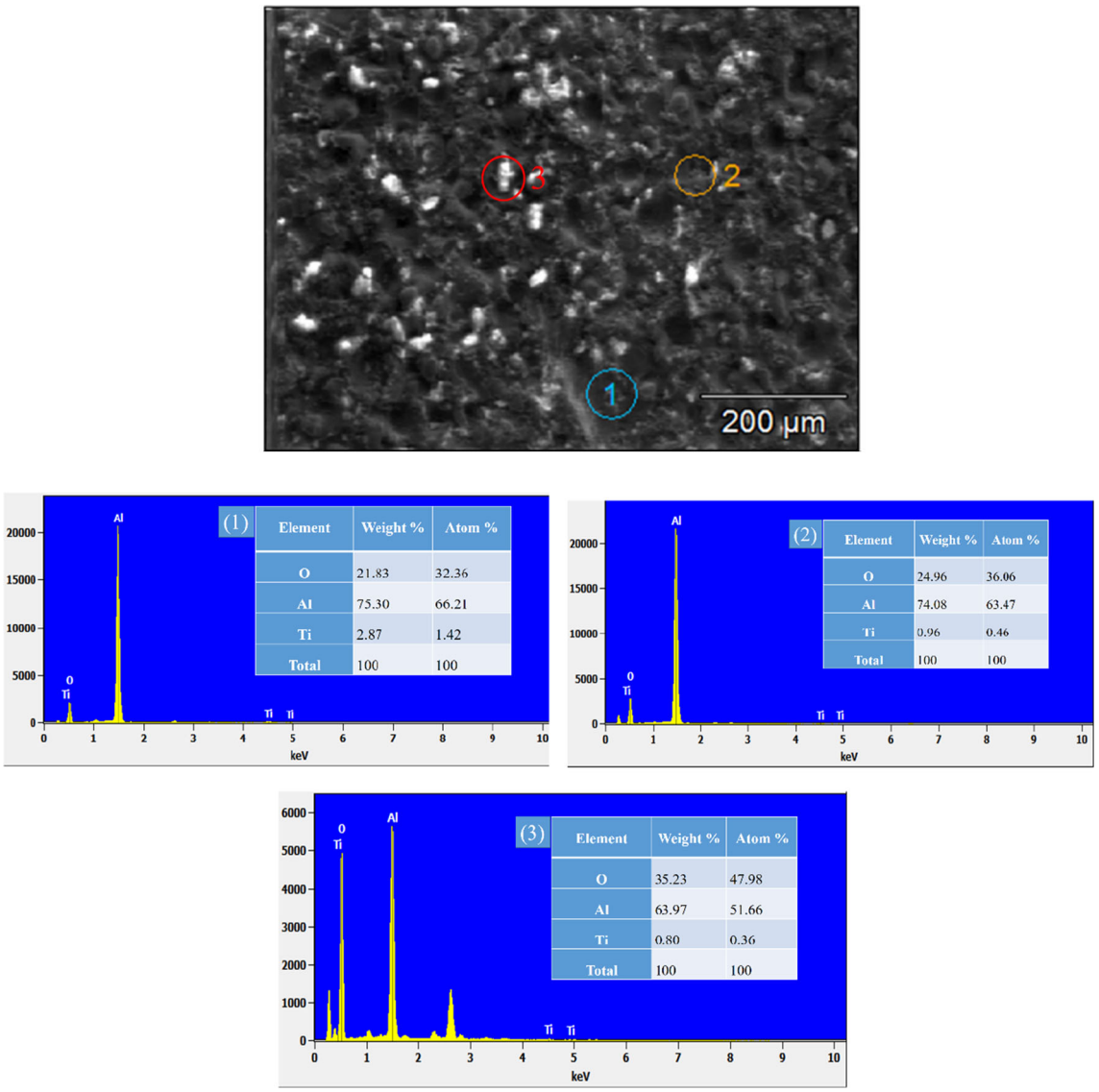

Fig. 8 SEM micrograph and EDS point analysis on three different locations of second-pass aluminum-reinforced TiO_2 particles **a** 1, **b** 2 and **c** 3

at the advancing side (AS) due to the insufficient materials flow and strain. The primary issue in the fabrication of the surface composites is agglomeration/clusters which is more pronounced in the case of addition of the submicron and nanolevel reinforcement. Multiple passes have been preferred for the breaking of clusters and distribution of particles in surface composites [15,16]. However, in our work, only two passes were implemented because the second FSP pass shows the marginal change in grain size and more homogenous microstructure when compared to the first pass. Additionally, we can able to achieve uniform distribution of particles within the stir zone as shown in Fig. 7d. It has been reported that FSP induces severe plastic deformation which results in grain refinement and homogeneity of as-cast A356 alloy [21]. Sharifitabar et al. [22] reported similar problems of agglomeration in the first pass of 5052Al/Al_2O_3 nanoparticle. Four FSP passes were carried out in same rotational direction for the dispersion of Al_2O_3 particles throughout the stir zone. At the same time, there may be a chance of formation of intermetallic because of the higher elevated temperature [23–26].

Figure 8 shows EDS point analysis at three different locations on surface composite; it reveals that the dark regions represent aluminum matrix and white region corresponds to TiO_2 particles. SEM micrographs reveal uniform distribution and good interfacial bonding between the particle and matrix. There is no sign of intermetallic compound. Three separate points of the matrix and particles are clearly visible in the SEM image, indicating the elements, such as Ti, Al, and O in these regions.

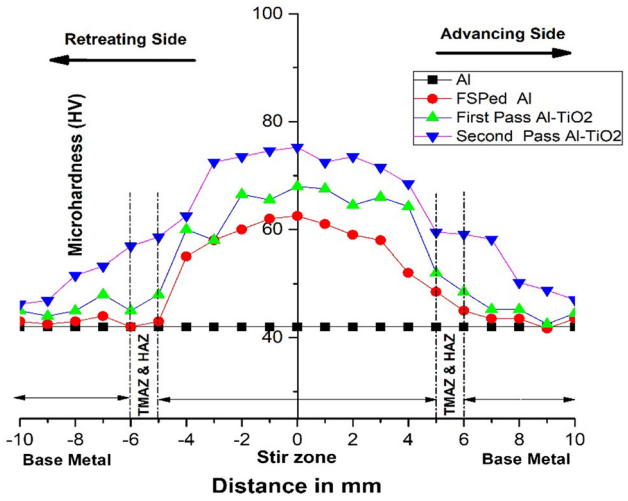

Fig. 9 Microhardness of aluminum and FSPed samples

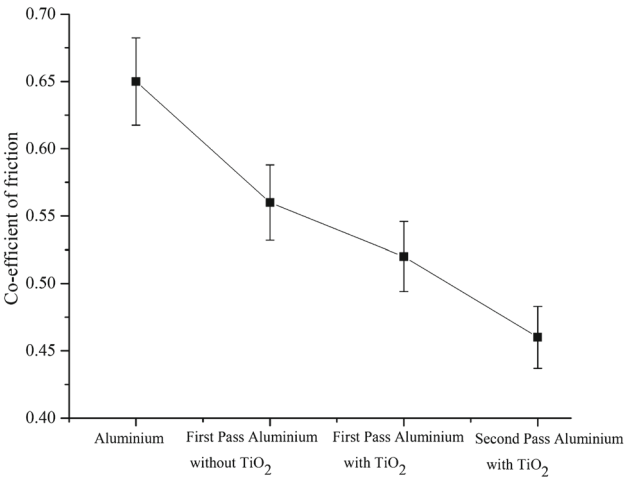

Fig. 10 Coefficient of friction of aluminum and FSPed samples

3.2 Microhardness

Figure 9 shows the hardness profile of base metal and FSPed samples. The average hardness of aluminum was found to be 42 HV. The improved hardness of second-pass surface composites is mainly due to the uniform dispersion of TiO_2 particles and dynamic recrystallization followed by grain refinement. However, the hardness of the first-pass surface composite shows marginal improvement when compared to FSPed aluminum without TiO_2, because of agglomerated particles and insufficient materials flow. Both grain size and hardness are interrelated, i.e., as grain size decreases, hardness increases and vice versa. The improved hardness of surface composite was also due to the thermal mismatch between TiO_2 particles and aluminum matrix leading to higher dislocation density. The uniform dispersion of particles in aluminum matrix results in pinning of dislocations and hinders grain growth. It has been reported that uniform

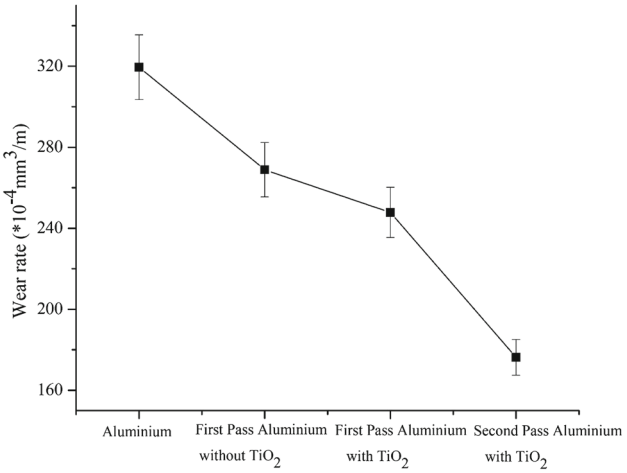

Fig. 11 Wear rate of aluminum and FSPed samples

dispersion of SiC particles in stir zone leads to the increase in the hardness value of the Al6061-SiC composite [12]. It has been reported nickel particles reinforced with Al1050 by friction stir processing show an average hardness of 50 HV compared to 29 HV for the Al [27].

3.3 Sliding Wear Behavior

The results of coefficient of friction and wear rate are carried out on the base metal, and FSPed samples are shown in Figs. 10 and 11, respectively. It is evident that uniform distribution of particles in the stir zone influences both the coefficient of friction (COF) and wear rates of surface composites. As seen in Fig. 10, it has been understood that the coefficient of friction decreases with an increase in FSP passes. The COF of base metal and the second-pass surface composites is found to be 0.65 and 0.46, respectively. It shows 30% decline in the friction coefficient of second-pass surface composites when compared with the base metal. The decrease in the coefficient of friction can be attributed to the deposition of a thin film of oxide on the counter disk. A similar observation has been reported in copper–hybrid composites [18].

Figure 11 represents the variations of the wear rate of the surface composite in comparison with aluminum. The surface composite exhibits lesser wear rate compared to the FSPed aluminum with and without particles and base metal because of the improved hardness and lubricating effect of the TiO_2 particles. There is a slight decrease in wear rate for first-pass surface composite compared to FSPed aluminum without particles. It is evident that agglomerated TiO_2 particles in the matrix have also contributed to reduce the wear rate. From Fig. 12a, it is observed that the morphology of the worn surface of base metal shows wide and shallow grooves, wear track covered with debris, heavy delamination and frac-

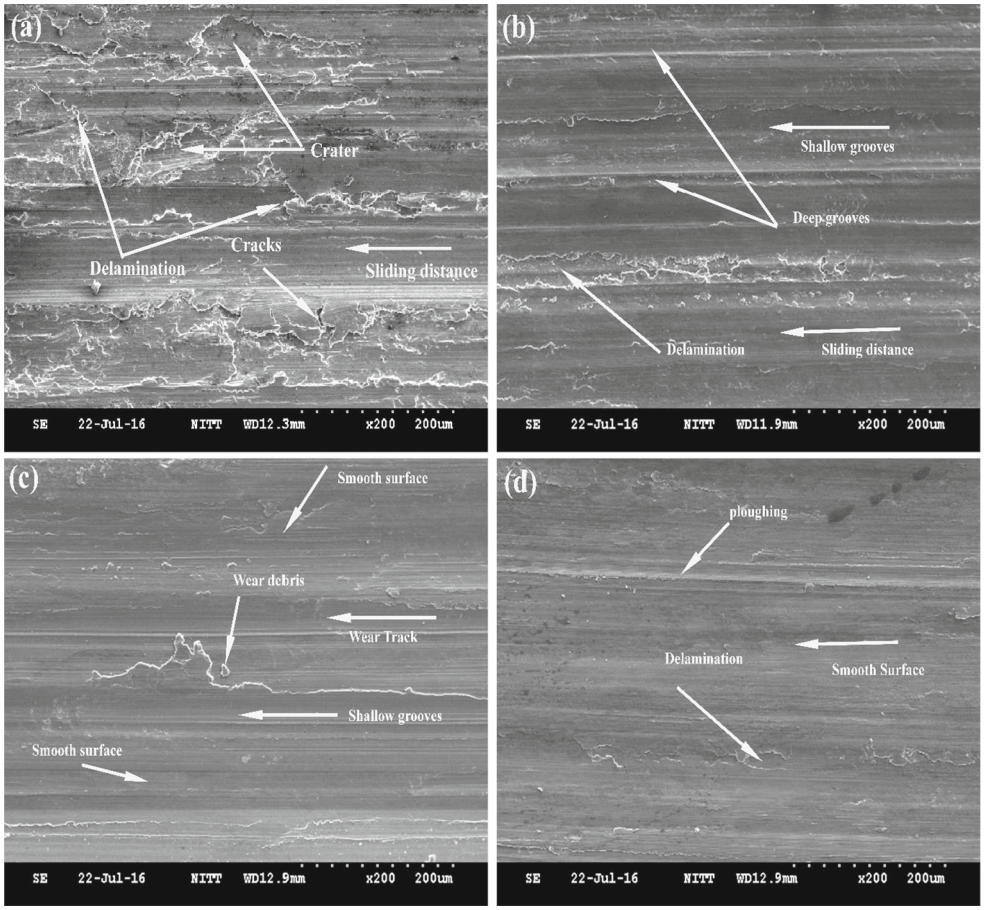

Fig. 12 SEM micrographs of worn surfaces of **a** aluminum, FSPed samples of **b** aluminum without TiO_2 particles **c** aluminum with TiO_2 particles, **d** second-pass aluminum with TiO_2 particles

ture of the transfer layer due to the plastic deformation of the base metal. The frictional heat generated between metal and disk contact surface will soften the base metal and remove the material in the form of debris. The SEM micrograph of shallow grooves and lesser debris are shown in Fig. 12b. It is evident that during FSP, the surface of base metal refined from the coarse grains to finer grains which in turn improves the hardness of base metal and hence hardness is inversely proportional to volumetric wear loss as per Archard model [28,29]. A similar trend was observed in the present work. Moreover, plowing mechanism leads to severe wear and initiate the abrasive type of wear and finally leads to the crack in the matrix resulting in delamination. In the surface composites, fine grooves were formed as shown in Fig. 12c, d. Surface composite does not have any significant loss of material because TiO_2 particles on the surface of aluminum come in contact with the counter disk, initially, have mild wear and then form a thin layer of the oxide film on specimens. Therefore, mechanically mixed layer (MML) was formed and hence reduces the wear rate of the surface composites. This is also due to the higher hardness of surface composite, resulting in the lower surface contact area.

4 Conclusions

In this study, titanium dioxide reinforced with aluminum surface composite layers was successfully fabricated using FSP. Microstructural evolution and tribological properties of the surface composite layers were investigated, and the following results were obtained:

1. The microstructure of the first pass with reinforcement exhibits cluster/agglomeration of particles at the advancing side due to insufficient materials flows and strain. However, the microstructure of the second pass with reinforcement reveals the acceptable distribution of particles by changing advancing and retreating side of aluminum plate without changes in process parameters.
2. The grain size of the surface composite samples processed by the second pass was observed to be finer due to the uniform distribution of particles leading to inhibition of grain growth in the friction stir zone.
3. Microhardness value for surface composites samples was higher with respect to aluminum, aluminum with and

without reinforcement because of uniform distribution of particles coupled with grain refinement.

4. The addition of TiO_2 particles improves the wear resistance of surface composites. The wear rate of base metal was found to be 319.5×10^{-4} mm^3/m and that of second-pass composite was found to be 176.3×10^{-4} mm^3/m. Therefore, second-pass composite enhances the wear resistance by 81% that of the base metal. Due to the uniform dispersion of TiO_2 particles, improved wear resistance also due to the grain refinement and formation of mechanically mixed layers played a significant role in reducing both coefficient of friction and wear rate.

Acknowledgements The author (Vikram Kumar S. Jain) would like to thank Department of Science and Technology, Government of India, for sponsoring him to pursue Ph.D. under INSPIRE Fellowship (DST/INSPIRE Fellowship/2015/IF150488).

References

1. Thomas, W.M.; Nicholas, E.D.; Needham, J.C.; Murch, M.G.; Templesmith, P.; Dawes, C.J.: Improvements to friction welding. GB Patent Application 9125978.8, 1991
2. Mishra, R.S.; Ma, Z.Y.: Friction stir welding and processing. Mater. Sci. Eng. R **50**, 1–78 (2005)
3. Li, J.Q.; Liu, H.J.: Effects of welding speed on microstructures and mechanical properties of AA2219-T6 welded by the reverse dual-rotation friction stir welding. Int. J. Adv. Manuf. Technol. **68**, 2071–2083 (2013)
4. Shen, J.J.; Liu, H.J.; Cui, F.: Effect of welding speed on microstructure and mechanical properties of friction stir welded copper. Mater. Des. **31**, 3937–3942 (2010)
5. Zhou, L.; Liu, H.J.; Liu, Q.W.: Effect of rotation speed on microstructure and mechanical properties of Ti–6Al–4V friction stir welded joints. Mater. Des. **31**, 2631–2636 (2010)
6. Lienert, T.J.; Stellwag Jr, W.L.; Grimmett, B.B.; Warke, R.W.: Friction stir welding studies on mild steel. Weld. J. Res. Suppl. **82**, 1s–9s (2003)
7. De, A.; Bhadeshia, H.K.D.H.; DebRoy, T.: Friction stir welding of mild steel: tool durability and steel microstructure. Mater. Sci. Technol. **30**, 1050–1056 (2014)
8. Watanabe, T.; Takayama, H.; Yanagisawa, A.: Joining of aluminum alloy to steel by friction stir welding. J. Mater. Process. Technol. **178**, 342–349 (2006)
9. Ma, Z.Y.; Mishra, R.S.; Mahoney, M.W.; Grimes, R.: High strain rate superplasticity in friction stir processed Al–Mg–Zr alloy. Mater. Sci. Eng. A **351**, 148–153 (2003)
10. Bauri, R.; Yadav, D.; Suhas, G.: Effect of friction stir processing (FSP) on microstructure and properties of Al–TiC in-situ composite. Mater. Sci. Eng. A **528**, 4732–4739 (2011)
11. Shahi, A.; Sohi, M.H.; Ahmadkhaniha, D.; Ghambari, M.: In situ formation of Al_3Ni composites on commercially pure aluminum by friction stir processing. Int. J. Adv. Manuf. Technol. **75**, 1331–1337 (2014)
12. D.H, Choi; Y Il, Kim; D.U,; S.B, Jung: Effect of SiC particles on microstructure and mechanical property of friction stir processed AA6061-T4. Trans. Nonferrous Met. Soc. China **22**, s614–s618 (2012)
13. Adel Mehraban, F.; Karimzadeh, F.; Abbasi, M.H.: Development of surface nanocomposite based on Al–Ni–O ternary system on Al6061 alloy by friction-stir processing and evaluation of its properties. JOM **67**, 998–1006 (2015)
14. Alidokht, S.A.; Abdollah-Zadeh, A.; Soleymani, S.; Assadi, H.: Microstructure and tribological performance of an aluminum alloy based hybrid composite produced by friction stir processing. Mater. Des. **32**, 2727–2733 (2011)
15. Yuvaraj, N.; Aravindan, S.: Vipin.: Wear characteristics of Al5083 surface hybrid nano-composites by friction stir processing. Trans. Indian Inst. Met. **70**, 1–19 (2016)
16. Khorrami, M.S.; Kazeminezhad, M.; Miyashita, Y.; Kokabi, A.H.: Improvement in the mechanical properties of Al/SiC nanocomposites fabricated by severe plastic deformation and friction stir processing. Int. J. Miner. Metall. Mater. **24**, 297–308 (2017)
17. Ding, Z.; Zhang, C.; Xie, L.; Zhang, L.-C.; Wang, L.; Lu, W.: Effects of friction stir processing on the phase transformation and microstructure of TiO_2-compounded Ti–6Al–4V Alloy. Metall. Mater. Trans. A **47**, 5675–5679 (2016)
18. Ramesh, C.S.; Noor Ahmed, R.; Mujeebu, M.A.; Abdullah, M.Z.: Fabrication and study on tribological characteristics of cast copper-TiO_2-boric acid hybrid composites. Mater. Des. **30**, 1632–1637 (2009)
19. Jain, V.K.S.; Muhammed, P.M.; Muthukumaran, S.; Babu, S.P.K.: Microstructure, mechanical and sliding wear behavior of AA5083–B4C/SiC/TiC surface composites fabricated using friction stir processing. Trans. Indian Inst. Met. **71**, 1519–1529 (2018)
20. Prado, R.; Murr, L.; Soto, K.; McClure, J.: Self-optimization in tool wear for friction-stir welding of Al 6061+ 20% Al_2O_3 MMC. Mater. Sci. Eng. A **349**, 156–165 (2003)
21. Arora, H.S.; Singh, H.; Dhindaw, B.K.: Composite fabrication using friction stir processing—a review. Int. J. Adv. Manuf. Technol. **61**, 1043–1055 (2012)
22. Madhusudhan Reddy, G.; Sambasiva Rao, A.; Srinivasa Rao, K.: Friction stir processing for enhancement of wear resistance of ZM21 magnesium alloy. Trans. Indian Inst. Met. **66**, 13–24 (2013)
23. Sharifitabar, M.; Sarani, A.; Khorshahian, S.; Shafiee Afarani, M.: Fabrication of 5052Al/Al_2O_3 nanoceramic particle reinforced composite via friction stir processing route. Mater. Des. **32**, 4164–4172 (2011)
24. Khayyamin, D.; Mostafapour, A.; Keshmiri, R.: The effect of process parameters on microstructural characteristics of AZ91/SiO_2 composite fabricated by FSP. Mater. Sci. Eng. A **559**, 217–221 (2013)
25. Khodabakhshi, F.; Simchi, A.; Kokabi, A.H.; Gerlich, A.P.; Nosko, M.: Effects of post-annealing on the microstructure and mechanical properties of friction stir processed Al–Mg–TiO_2 nanocomposites. Mater. Des. **63**, 30–41 (2014)
26. Sharma, V.; Prakash, U.; Kumar, B.V.M.: Surface composites by friction stir processing: a review. J. Mater. Process. Technol. **224**, 117–134 (2015)
27. Yadav, D.; Bauri, R.: Processing, microstructure and mechanical properties of nickel particles embedded aluminum matrix composite. Mater. Sci. Eng. A **528**, 1326–1333 (2011)
28. Ramesh, C.S.; Khan, A.R.A.; Ravikumar, N.; Savanprabhu, P.: Prediction of wear coefficient of Al6061–TiO_2 composites. Wear **259**, 602–608 (2005)
29. Jerome, S.; Ravisankar, B.; Kumar Mahato, P.; Natarajan, S.: Synthesis and evaluation of mechanical and high-temperature tribological properties of in-situ AlTiC composites. Tribol. Int. **43**, 2029–2036 (2010)